Chromatic Dispersion Monitoring of CSRZ Signal for Optimum Compensation Using Extracted Clock-Frequency Component

Sung-Man Kim and Jai-Young Park

This paper presents a chromatic dispersion monitoring technique using a clock-frequency component for carrier-suppressed return-to-zero (CSRZ) signal. The clock-frequency component is extracted by a clock-extraction (CE) process. To discover which CE methods are most efficient for dispersion monitoring, we evaluate the monitoring performance of each extracted clock signal. We also evaluate the monitoring ability to detect the optimum amount of dispersion compensation when optical nonlinearity exists, since it is more important in nonlinear transmission systems. We demonstrate efficient CE methods of CSRZ signal to monitor chromatic dispersion for optimum compensation in high-speed optical communication systems.

Keywords: Carrier-suppressed return-to-zero (CSRZ), clock component, chromatic dispersion monitoring, optical nonlinearity, optimum dispersion compensation.

Manuscript received Jan. 23, 2007; revised Jan. 10, 2008.

Sung-Man Kim (phone: + 82 31 279 4361, email: sammouse@gmail.com) and Jai-Young Park (email: jypark2@samsung.com) are with Network R&D Center, Samsung Electronics, Suwon, Gyeonggi-do, Rep. of Korea.

I. Introduction

In high-speed optical communication systems with ≥40 Gb/s per channel, it is essential to monitor and compensate in real time for chromatic dispersion that can be changed by temperature variation [1] or dynamic reconfiguration of the optical network. In fact, the future emergence of optical systems with ≥40 Gb/s per channel depends on an understanding and development of robust solutions for tunable dispersion compensation [2]. A key element of tunable dispersion compensation is chromatic dispersion monitoring. There have been substantial efforts to develop effective chromatic dispersion monitoring techniques. The previous works on chromatic dispersion monitoring include techniques based on a clock-frequency (bit-rate frequency) component [3]-[6], phase-modulation to amplitude-modulation conversion [7], [8], and subcarrier tone [9], [10]. Among the existing techniques, the technique based on clock signal seems to be the simplest because it does not need the addition of any extra modulation to the data signal.

However, the clock-based monitoring technique has a disadvantage of being dependent on signal modulation format. For instance, the characteristic of a return-to-zero (RZ) clock in relation to dispersion is quite different from that of a non return-to-zero (NRZ) clock [4]. Therefore, to use a clock-based monitoring technique in newly-developed modulation formats such as carrier-suppressed RZ (CSRZ) [11]-[13], it is necessary to investigate the characteristic of the clock component on specific modulation formats.

The CSRZ format has better spectral efficiency and robustness

to dispersion than the RZ format [12]; therefore, it is widely used for demonstrating high-speed optical communication systems [13]. However, the characteristic of the original CSRZ clock does not seem suitable for chromatic dispersion monitoring because its dispersion behavior resembles a ripple [5]. In this paper, we demonstrate that the characteristic of the CSRZ clock can be changed by using a clock-extraction (CE) process. We also demonstrate that the changed clock characteristic can be quite suitable for chromatic dispersion monitoring.

In addition to chromatic dispersion monitoring, nonlinear distortion monitoring is important for optimum dispersion compensation. In real high-speed optical communication systems with ≥40 Gb/s per channel, a high optical signal power is used to satisfy the required optical signal-to-noise ratio. In this case, the optical nonlinearity induced by the high optical signal power shifts the optimum amount of dispersion compensation [14]. For this reason, we also investigate the monitoring ability of CE methods to detect the optimum amount of dispersion compensation when optical nonlinearity exists. As a result, we find out which CE methods are most efficient to monitor chromatic dispersion for optimum compensation in high-speed communication systems. We have carried out similar work for the case of NRZ signal [6].

II. Clock Extraction

1. Original CSRZ Clock

The CSRZ signal format uses two Mach-Zehnder modulators; one is driven by the 40-Gb/s data signal, and the other is driven by 20-GHz sinusoidal signal [10]. Using modeling, we simulated optical and electrical spectra of CSRZ signal, as shown in Fig. 1. Spectra of RZ signal are also shown in Fig. 1 for comparison. Although the optical spectrum of CSRZ signal, unlike that of RZ signal, does not have a discrete carrier frequency (this is why this signal format is called *carrier-suppressed* RZ), its electrical spectrum has a discrete DC frequency and a clock-frequency component as RZ signal does.

The two frequency components in the optical spectrum, f and $f+fc$, generate the frequency component, fc, in the electrical spectrum due to the square characteristic of the photo diode (PD). In other words, an electrical spectrum after PD originates from the beat of the optical spectrum. Chromatic dispersion causes linear phase difference in the optical spectrum along the frequency. This phase difference results in the amplitude degradation of a frequency [15]. This is why chromatic dispersion causes clock power padding.

The clock-frequency component of CSRZ signal in the electrical spectrum is mainly caused by the beat of the two

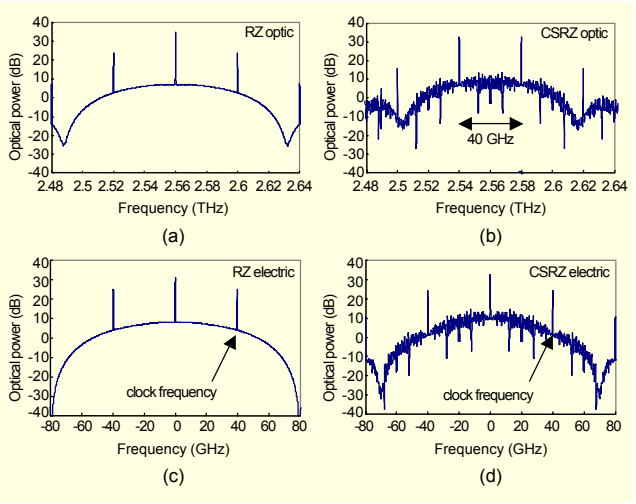

Fig. 1. Optical spectra of (a) 40-Gb/s RZ and (b) 40-Gb/s CSRZ, and electrical spectra of (c) 40-Gb/s RZ and (d) 40-Gb/s CSRZ. Electrical Spectra were obtained after a photo-diode receiver.

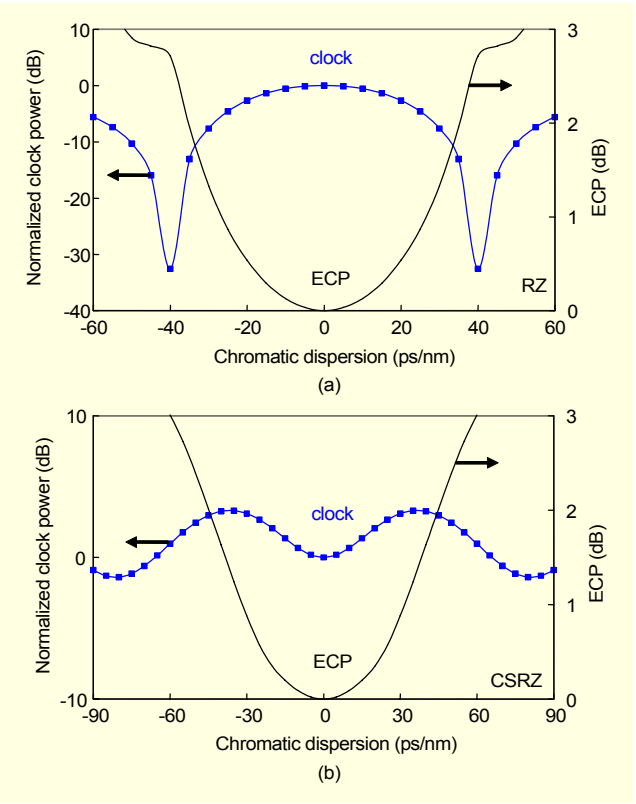

Fig. 2. Clock power and ECP as a function of chromatic dispersion: (a) 40-Gb/s RZ signal and (b) 40-Gb/s CSRZ signal. Note that the scales of Y-axes are different.

discrete frequency components in the optical spectrum, which are separated by 40 GHz, as shown in Fig. 1(b).

Figure 2 shows the RF clock power of RZ and CSRZ signals as a function of chromatic dispersion. In this paper, eye-closure

penalty (ECP) is defined as

$$ECP(\text{dB}) = 10\,\text{Log}_{10}\left(\frac{eye\ opening\ w/o\ dispersion}{eye\ opening\ w/\ dispersion}\right).$$

The RZ clock has been widely used for chromatic dispersion monitoring, since its dispersion behavior is monotonic and its monitoring range and sensitivity are quite good for chromatic dispersion monitoring [3], [4]. The monitoring range of the RZ clock is 40 ps/nm, which corresponds to an ECP of > 2 dB. The power change of the RZ clock within the monitoring range is over 30 dB. However, the CSRZ clock does not seem to be suitable for chromatic dispersion monitoring, since its dispersion behavior resembles a ripple. The monitoring range of the original CSRZ clock is about 35 ps/nm, which corresponds to an ECP of only 1 dB. The power change of the CSRZ clock within the monitoring range is less than 5 dB; therefore, other techniques may be required to monitor chromatic dispersion in CSRZ signal.

2. CE Methods for CSRZ Signal

Although the original CSRZ clock does not seem to be suitable for chromatic dispersion monitoring, the characteristic of the CSRZ clock can be changed by using a CE process. We investigated various CE methods as shown in Fig. 3 [6]. We consider a CE scheme consisting of spectrum processing, nonlinear processing, and a band-pass filter (BPF). We consider $r(t)$, $r(t)$–$r(t–T/2)$, and $r(t)$+$r(t–T/2)$ as the spectrum processing functions, where $r(t)$ is a received ac-coupled signal and T is one-bit period. Here, $r(t)$–$r(t–T/2)$ functions as a high-pass filter within the bit-rate bandwidth, and $r(t)$ + $r(t–T/2)$ functions as a low-pass filter within the bit-rate bandwidth, as shown in Fig. 4. We consider x, x^2, $D(x)$, and $RD(x)$ as the nonlinear processing functions, where x is the input of the nonlinear processing, $D(x)$ is a diode function, and $RD(x)$ is a reverse diode function (= $–D(–x)$). Their transfer functions and implementations are shown in Fig. 5. After passing through the nonlinear processing, the characteristic of the clock component is changed. Then, a discrete clock frequency is extracted by using the BPF whose center frequency is the bit-rate frequency.

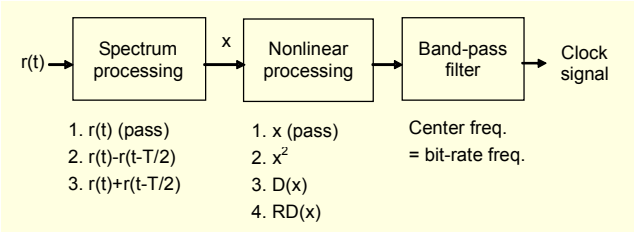

Fig. 3. CE scheme for CSRZ signal: $r(t)$ is a received ac-coupled CSRZ signal, T is one-bit period, $D(x)$ is a diode function ($D(x) = x$ if $x \geq 0$ and $D(x) = 0$ if $x < 0$), and RD is a reverse diode function ($RD(x) = -D(-x)$).

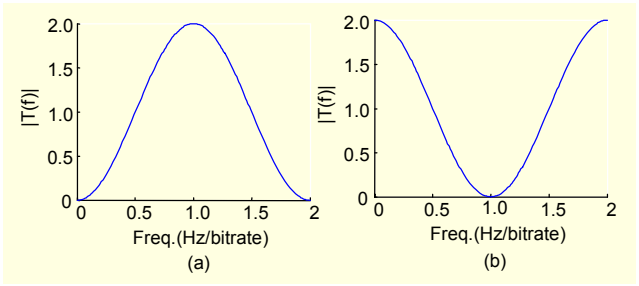

Fig. 4. Transfer functions of the spectrum processing: (a) $r(t)$-$r(t$-$T/2)$ and (b) $r(t)$ + $r(t$-$T/2)$.

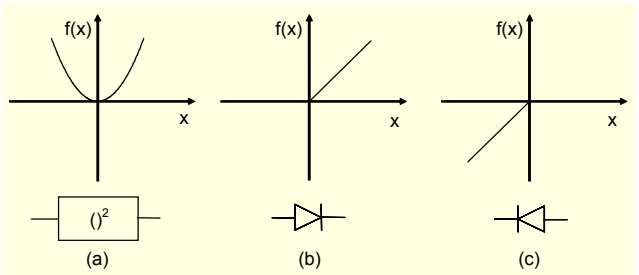

Fig. 5. Transfer functions of nonlinear processing: (a) x^2, (b) $D(x)$, and (c) $RD(x)$.

Table 1. CE methods for CSRZ signal.

Spectrum processing	Nonlinear processing	Method
r(t) (pass)	x (pass)	M1
r(t) (pass)	x^2	M2
	D(x)	M3
	RD(x)	M4
r(t)-r(t-T/2) (HPF)	x^2	M5
	D(x)	M6
	RD(x)	M7
r(t)+r(t-T/2) (LPF)	x^2	M8
	D(x)	M9
	RD(x)	M10

Table 1 shows a summary of the CE methods considered in this paper. The CE methods are denoted as M1 to M10, according to the spectrum processing function and the nonlinear processing function. The CE method M1 is the original CSRZ clock. The CE methods M5 and M8 are theoretically identical methods and so are M9 and M10. All the CE methods in Table 1 can be easily implemented.

3. Spectral Explanation for CE Process

Some CE methods in Table 1 can be explained easily in the

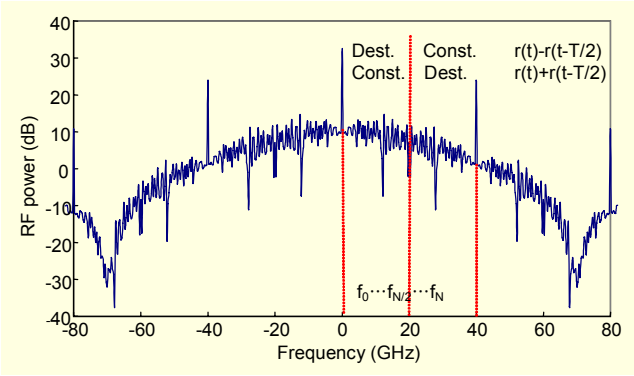

Fig. 6. Effect of spectrum processing functions on the signal spectrum.

spectral domain, especially the CE methods using square processing (M2, M5, and M8). The CE methods using diode and reverse diode processing (M3/4, M6/7, and M9/10) are difficult to explain in the spectral domain, so they will not be covered in this part.

Figure 6 shows the electrical spectrum of the CSRZ signal. For the square methods, the extracted clock-frequency component f_{clock} originates from the beat between f_i and f_{N-i}. Therefore, the extracted clock-frequency component can be expressed as

$$f_{clock} \cong \sum_{i=0}^{N/2} f_i \times f_{N-i} \ , \qquad (1)$$

where f_0 and f_N are the frequency component at 0 Hz and the clock frequency, respectively. That is, the extracted clock-frequency component is the result of the multiplication of the two frequencies which are the same frequency distance from the half clock (f_{clock} / 2).

Figure 6 also indicates the effect of spectrum processing on the signal spectrum. The spectrum processing function, $r(t) - r(t - T/2)$, causes destructive interference on the low-frequency part and constructive interference on the high-frequency part. Meanwhile, the spectrum processing function, $r(t) + r(t - T/2)$, gives constructive interference on the low-frequency part and destructive interference on the high-frequency part. Thus, the effect of the two spectrum processing functions, $r(t) - r(t - T/2)$ and $r(t) + r(t - T/2)$, are symmetrical to the half clock as shown in Fig. 4. In other words, the effect of $r(t) - r(t - T/2)$ on f_i is equal to that of $r(t) + r(t - /2)$ on f_{N-i}, and vice versa. The square function can be used to obtain the clock frequency by multiplying two frequencies (f_i and f_{N-i}), which are symmetrically distanced from the half clock. Thus, the two CE methods, M5 (square after $r(t) - r(t - T/2)$) and M8 (square after $r(t) + r(t - T/2)$), yield identical results.

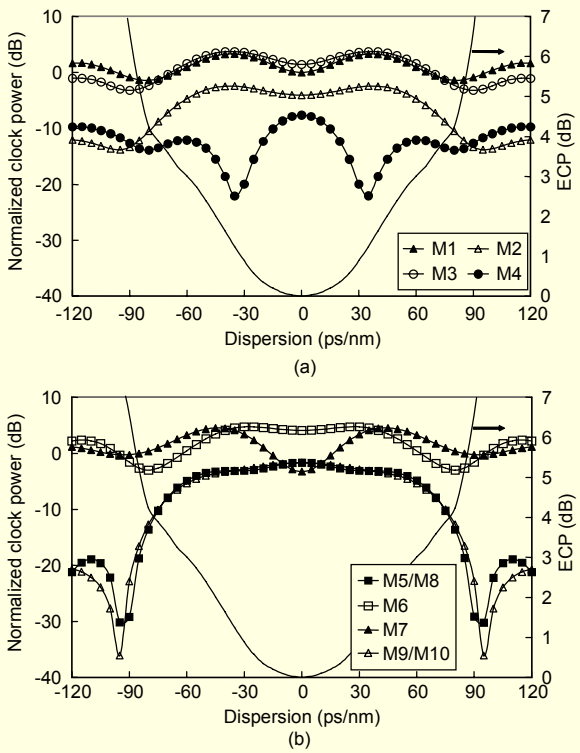

Fig. 7. Clock power extracted by each CE method. Solid line is the ECP of the 40-Gb/s CSRZ signal. M1 is the original CSRZ clock. (a) M1 to M4 and (b) M5 to M10.

III. Chromatic Dispersion Monitoring

1. Criteria for Performance Comparison

Figure 7 shows the simulation result of the clock power extracted by each CE method as a function of chromatic dispersion. Different CE methods yield different clock characteristics.

In the simulation, we tried to model the real transmitter and receiver. The input signal is a 40-Gb/s pseudorandom binary sequence (PRBS) of 2^7-1. Note that we could not find any serious difference in the results of simulations conducted with other PRBS lengths. Although it requires more simulation time, we decided to conduct our simulations with a PRBS length of 2^7-1 to achieve more accurate results. The bandwidths of the transmitter and the receiver are 40 and 30 GHz, respectively. The bandwidth of the receiver optical filter is 60 GHz with the fifth-order Butterworth filter shape. We evaluated the CE methods by two criteria: monitoring range and sensitivity. The monitoring range and sensitivity are defined as shown in Fig. 8. The monitoring range is defined as the dispersion window up to which the clock power decreases (or increases) monotonically. A wider monitoring range is preferable. Sensitivity is defined as the power change of the clock per unit

Table 2. Performance comparison for chromatic dispersion monitoring.

CE method	Monitoring range (ps/nm)	Sensitivity (dB/ps/nm,@ D=0)	Total evaluation
M1	±35 (bad)	0.06	Bad
M2	±35 (bad)	0.02	Bad
M3	±35 (bad)	0.04	Bad
M4	±35 (bad)	0.10	Bad
M5/M8	±95	0.03	Good
M6	±25 (bad)	0.02	Bad
M7	±45	0.14	Good
M9/M10	±95	0.02	Good

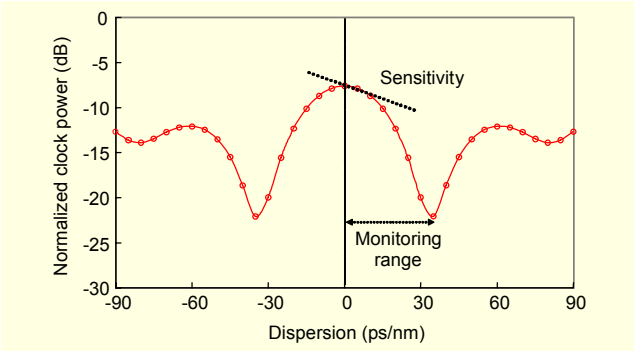

Fig. 8. Definition of monitoring range and sensitivity.

dispersion. Sensitivity is meaningful at near zero dispersion assuming a feedback control to minimize dispersion penalty. Thus, we defined the sensitivity of the CE methods as the clock power change in the range from 0 to10 ps/nm. Since higher sensitivity gives higher monitoring accuracy, the CE method with high sensitivity is better than others.

2. Results and Discussion

From the simulation results in Fig. 7, we obtain the monitoring range and sensitivity of the CE methods. They are summarized in Table 2. We consider that the monitoring range may need to be > 35 ps/nm at 40 Gb/s, which induces 1-dB ECP. With this consideration, we chose M5/8, M7, and M9/10 as good CE methods for chromatic dispersion monitoring. Among the good CE methods, a CE method can be chosen according to the desired system requirement. In a system in which the monitoring range is more important, M5/8 or M9/10 can be chosen because they yield the widest monitoring range. In a system in which monitoring accuracy is more important, M7 can be chosen because M7 yields the best sensitivity. By combining the two CE methods that yield the widest monitoring range and the best sensitivity, the chromatic dispersion monitoring technique based on the clock component could meet most system requirements.

IV. ODC Monitoring

1. ODC Estimation Error

One of the main purposes of dispersion monitoring is to use its output as a feedback control signal for a tunable dispersion compensator. In this scenario, a dispersion monitor should be able to detect the optimum amount of dispersion compensation even if optical nonlinearity shifts it; we call it *optimum dispersion compensation* (*ODC*) *monitoring*. In the ideal linear transmission system, the optimum dispersion-compensation ratio (DCR) is 100% and the clock power is maximal (or minimal) at the 100% DCR. Thus, we can compensate for chromatic dispersion optimally so as to maximize (or minimize) the clock power. However, in the real nonlinear transmission case where most 40-Gb/s systems are included, the optimum DCR is shifted due to the effect of self-phase modulation [14]. In this nonlinear transmission case, the DCR showing the peak clock power is also shifted. An example of the ECP and clock power in the real nonlinear transmission is shown in Fig. 9. As shown in Fig. 9(a), the ODC point of the nonlinear case is nearly 100% DCR, in contrast with the NRZ case [6]. Previous researchers have reported similar results [16].

In the nonlinear transmission case, we define the ODC estimation error of the CE methods in order to estimate the ODC monitoring ability. It is defined as the difference between the ECP at the ODC and the ECP at the DCR showing the peak clock power, as shown in Fig. 10. In other words, ODC estimation error is the penalty incurred when we compensate dispersion so as to maximize (or minimize) the clock power. If the ODC estimation error of a CE method is below a required value (such as 1 dB), the CE method can be used for ODC monitoring.

2. Transmittable Condition

Using numerical simulations, we can investigate the ODC estimation error of the CE methods. However, unlike linear simulation, nonlinear simulation results are dependent on many simulation parameters, such as optical signal power, transmission length, and fiber dispersion. Therefore, we need to set the range of nonlinear simulation condition. Since it is unnecessary to consider the simulation condition where a data signal cannot be transmitted properly, we confine our interest to the proper transmittable condition, as shown in Fig. 11. There are two requirements for proper optical transmission.

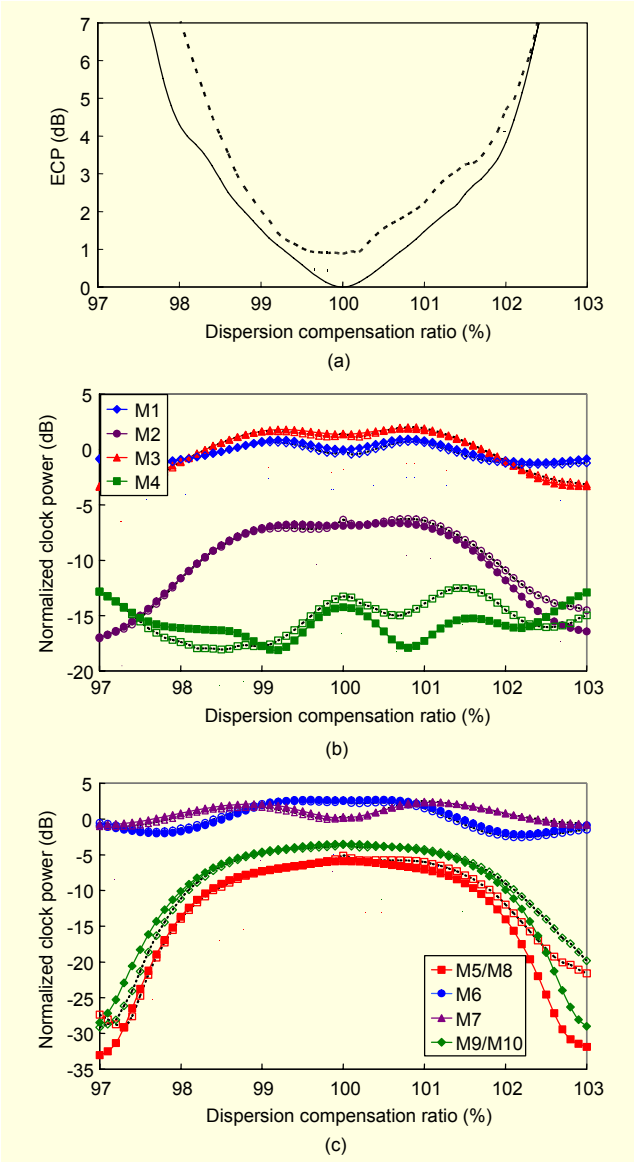

Fig. 9. Nonlinear simulation results at 960-km NZDSF transmission with a signal power of -3 dBm. Solid shapes are the linear transmission case and hollow shapes are the nonlinear transmission case: (a) ECP of the received signal, (b) clock power extracted with M1 to M4, and (c) clock power extracted with M5 to M10.

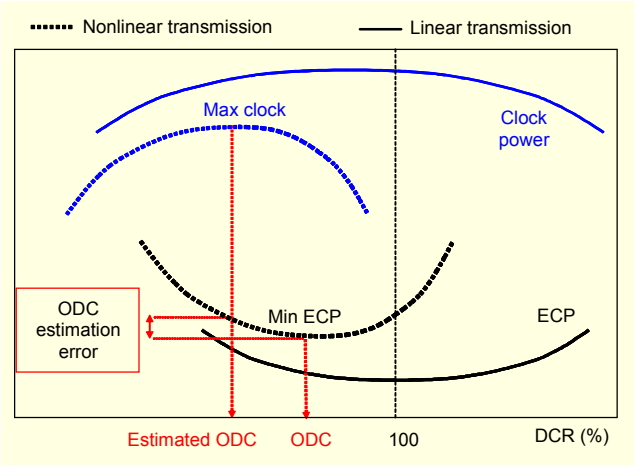

Fig. 10. Definition of ODC estimation error. The solid line is a linear transmission case and the dashed line is a nonlinear transmission case.

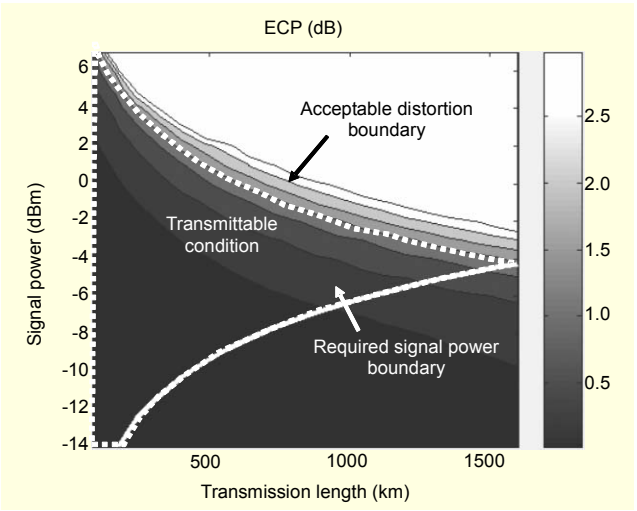

Fig. 11. Definition of transmittable condition. Each ECP value in the plot is the minimum ECP at ODC.

First, the optical signal power should be high enough to satisfy the required optical signal-to-noise ratio (26.7 dB for a bit-error rate of 10^{-15} at 40 Gb/s) at the receiver. The required signal power curve is calculated with the equation in [17], assuming a 5-dB coding gain of forward error correction. Second, the signal power should be low enough not to create severe nonlinear distortion. Even if dispersion is compensated optimally, signal distortion is not completely eliminated due to optical nonlinearities [14]. We consider signal distortion showing the minimum ECP of <1 dB acceptable. The acceptable nonlinear distortion boundary is obtained by using numerical simulations, as shown in Fig. 11. To investigate the minimum ECP at each point on the plot, we conducted several nonlinear simulations varying the dispersion compensation (0.1% DCR step) for each optical power (1-dB step). In the simulations, we assumed the use of nonzero dispersion-shifted fiber (NZDSF, D = 4 ps/nm/km) and Raman amplifiers with 80-km span length. We adjusted the Raman pumping powers to compensate the loss of each span. We also assumed that dispersion is compensated at each span by dispersion-compensating fiber (DCF).

3. Results and Discussion

Using numerical simulations, we investigated the ODC estimation error of the CE methods in the 40-Gb/s transmission

Table 3. Performance comparison for ODC monitoring.

CE method	Monitoring range (ps/nm)	Sensitivity (dB/ps/nm, @ D=0)	Estimation error (dB)	Total evaluation
M1	±30 (bad)	0.03	< 0.3	Bad
M2	-25 to 30 (bad)	0.001	< 0.5	Bad
M3	±30 (bad)	0.02	< 0.3	Bad
M4	-30 to 25 (bad)	0.09	< 0.3	Bad
M5/8	±95	0.03	< 0.3	Choice 1
M6	-20 to 15 (bad)	0.01	< 1.0	Bad
M7	-40 to 35 (bad)	0.05	< 0.3	Bad
M9/10	±95	0.02	< 0.3	Choice 2

system. We assumed the use of NZDSF (D = 4 ps/nm/km) and Raman amplifiers with 80-km span length. We also assumed five-channel wavelength-division-multiplexing transmission with 100-GHz channel spacing to consider the effects of cross-phase modulation and four-wave mixing.

We obtained the monitoring range, sensitivity, and ODC estimation error for the whole transmittable condition as summarized in Table 3. From these results, we conclude that M5/8 and M9/10 can be used to monitor ODC in the real nonlinear transmission system. We also confirmed the ODC monitoring ability of M5/8 and M9/10 in the case of the standard single-mode fiber (D=17 ps/nm/km) system, although we do not show the results in this paper.

V. Conclusion

This paper presented a chromatic dispersion monitoring technique using a clock-frequency component for CSRZ signal. We demonstrated that efficient CE methods that can be used in chromatic dispersion monitoring of CSRZ signal. We also showed that our technique can be used to find the optimum dispersion compensation in the nonlinear transmission system. Our simulation results demonstrate that the clock component extracted by the CE methods denoted as M5/8 ($= [r(t) \pm r(t - T/2)]^2$) and M9/10 ($= D[r(t) + r(t - T/2)]$ or $RD[r(t) + r(t - T/2)]$) are useful to monitor chromatic dispersion and optimum compensation in high-speed optical transmission systems.

References

[1] T. Kato, Y. Koyano, and M. Nishimura, "Temperature Dependence of Chromatic Dispersion in Various Types of Optical Fibers," *Proceeding of Optical Fiber Communication Conference (OFC),* paper TuG7, 2000.

[2] I. Kaminow and T. Li, *Optical Fiber Telecommunications IV B*, Chapter 14, Academic Press, 2002, pp. 703-707.

[3] G. Ishikawa and H. Ooi, "Demonstration of Automatic Dispersion Equalization in 40 Gbit/s OTDM Transmission," *Proceeding of European Conference on Optical Communication (ECOC)*, Madrid, Spain, Sept. 1998, pp. 519-520.

[4] Z. Pan, Q. Yu, Y. Xie, S.A. Havstad, A.E. Willner, D.S. Starodubov, and J. Feinberg, "Chromatic Dispersion Monitoring and Automated Compensation for NRZ and RZ Data Using Clock Regeneration and Fading without Adding Signaling," *Proc. Optical Fiber Communication Conference (OFC)*, CA, Paper WH5, 2001.

[5] S.M. Reza, M. Nezam, T. Luo, J.E. McGeehan, and A.E. Willner, "Enhancing the Monitoring Range and Sensitivity in CSRZ Chromatic Dispersion Monitors Using a Dispersion-Biased RF Clock Tone," *IEEE Photon. Technol. Lett.*, vol. 16, no. 5, 2004, pp. 1391-1393.

[6] S.M. Kim and C.H. Lee, "The Efficient Clock-Extraction Methods of NRZ Signal for Chromatic Dispersion Monitoring," *IEEE Photon. Technol. Lett.*, vol. 17, no. 5, 2005, pp. 1100-1102.

[7] S. Kuwahara, A. Sano, K. Yonenaga, Y. Miyamoto, and H. Toba, *Electronics Lett.*, "Simple Zero Dispersion Detection Technique Using Alternating Chirp Signal in Automatic Dispersion Equalization System," vol. 35, no. 7, 1999, pp. 593-594.

[8] A.R. Chraplyvy, R.W. Tkach, L.L. Buhl, and R.C. Alferness, "Phase Modulation to Amplitude Modulation Conversion of CW Laser Light in Optical Fibers," *Electronics Lett.*, vol. 22, no. 8, Apr. 1986, pp. 409-411.

[9] M.N. Petersen, Z. Pan, S. Lee, S.A. Havstad, and A.E. Willner, "Dispersion Monitoring and Compensation Using a Single Inband Subcarrier Tone," *Proc. Optical Fiber Communication Conference (OFC)*, Anaheim, CA, Paper WH4, 2001.

[10] G. Rossi, T.E. Dimmick, and D.J. Blumenthal, "Optical Performance Monitoring in Reconfigurable WDM Optical Networks Using Subcarrier Multiplexing," *J. Lightwave Technol.*, vol. 18, no. 12, Dec. 2000, pp. 1639-1648.

[11] A. Sano and Y. Miyamoto, "Performance Evaluation of Prechirped RZ and CS-RZ Formats in High-Speed Transmission Systems with Dispersion Management," *J. Lightwave Technol*,, vol. 19, no. 12, 2001, pp. 1864-1871.

[12] Y. Miyamoto, T. Kataoka, K. Yonenaga, M. Tomizawa, A. Hirano, S. Kuwahara, and Y. Tada, "WDM Field Trials of 43-Gb/s/Channel Transport System for Optical Transport Network," *J. Lightwave Technol*, vol. 20, no. 12, 2002, pp. 2115-2128.

[13] M. Jaworski, "Optical Modulation Formats for High-Speed DWDM Systems," *Proceeding of International Conference on Transparent Optical Networks (ICTON)*, paper We.P.21, 2003, pp. 162-165.

[14] I. Kaminow and T. Li, *Optical Fiber Telecommunications IV B*, Academic Press, 2002, pp. 613-617.

[15] D. Derickson, *Fiber Optic Test and Measurement*, Prentice Hall,

Inc., 1998, pp. 486-487.
[16] A. Hirano, Y. Miyamoto, K. Yonenaga, A. Sano, and H. Toba, "40 Gbit/s L-Band Transmission Experiment Using SPM-Tolerant Carrier-Suppressed RZ Format," *Electronics Letters*, vol. 35, no. 25, 1999, pp. 2213-2215.
[17] I. Kaminow and T. Li, *Optical Fiber Telecommunications IV A*, Academic Press, 2002, p. 20.

Sung-Man Kim received the BS, MS, and PhD degrees in electrical engineering from Korea Advanced Institute of Science and Technology (KAIST), Daejeon, Rep. of Korea, in 1999, 2001, and 2006, respectively. His main interests during the PhD course included chromatic dispersion monitoring. In 2006, he joined the network R&D center of Samsung Electronics in Suwon, Rep. of Korea, where he worked on the research and development of optical access networks. He is currently a senior engineer at Samsung Electronics. His research interests include optical performance monitoring and passive optical networks.

Jai-Young Park received the BS degree in electronics engineering from Kwangwoon University, Seoul, Rep. of Korea, in 1989. He is currently working toward a MS degree with the Department of Electrical Engineering of Sungkyunkwan University, Suwon, Rep. of Korea. His main interests include Ethernet passive optical networks. From 1989 to 1994, he was an engineer at Datacomm, Seoul, Rep. of Korea, where he worked on the design of dial-up and leased line modems. In 1994, he joined the network R&D center of Samsung Electronics, Suwon, Rep. of Korea, where he worked on the research and development of SDH/SONET, xDSL, and optical access networks. He is currently a principal engineer at Samsung Electronics. His research interests include passive optical networks and broadband convergence networks.